STATUS OF BEAM IMAGING DEVELOPMENTS FOR THE SNS TARGET

T. J. Shea, C. Maxey, T. J. McManamy, ORNL, Oak Ridge, Tennessee, USA
D. Feldman, R. Fiorito, A. Shkvarunets , UMD, College Park, Maryland, USA

Abstract

The Spallation Neutron Source (SNS) continues a ramp up in proton beam power toward the design goal of 1.4 MW on target. At Megawatt levels, US and Japanese studies have shown that cavitation in the Mercury target could lead to dramatically shortened target lifetime. Therefore, it will be critical to measure and control the proton beam distribution on the target, in a region of extremely high radiation and limited accessibility. Several sources of photons have been considered for imaging the beam on or near the target. These include a freestanding temporary screen, a scintillating coating, Helium gas scintillation, optical transition radiation, and a beam-heated wire mesh. This paper will outline the selection process that led to the current emphasis on coating development. In this harsh environment, the optics design presented significant challenges. The optical system has been constructed and characterized in preparation for installation. Optical test results will be described along with predictions of overall system performance.

MOTIVATION

The design of targets for megawatt class accelerators is generally limited by material issues such as radiation damage, the ability to adequately cool the structures and the stresses generated by thermal profiles, coolant pressures and short pulse effects. Performance usually improves with more compact targets, while the engineering challenges increase. A key parameter for design is the beam profile and peak current density for a given beam energy since this drives the peak radiation damage rate, the peak volumetric heating in the target and the peak heating in any window system the beam passes through. The containment structure for liquid metal targets are also subject to cavitation damage for short pulse operation and studies for SNS and JSNS mercury targets have shown this may be a sensitive function of peak current density [1]. Generally, targets that are designed for high performance are close to the engineering limits and subject to potential damage if the beam density or power increases. Development of diagnostic systems which give accurate beam profile information during full power operation would allow targets to be safely designed with less engineering margin and with improved lifetime estimates based on radiation damage. Rapid detection of high beam density could be used to trip the beam for target protection.

As shown in Fig. 1, the SNS will operate at beam powers exceeding 1 MW by late 2009. Currently, from a location 9.5 meters upstream of the target, a harp provides the last profile measurement. This multi-wire device and upstream instrumentation provide data that help predict the properties of the beam at the target. Unfortunately, the
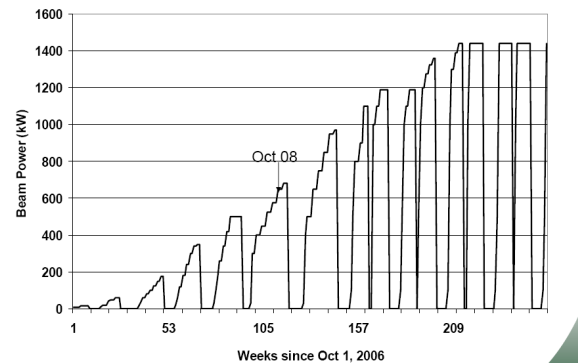
Figure 1: Ramp-up of SNS beam power.

estimated uncertainty of the current density prediction exceeds 25%. Assuming that the target's damage rate scales with the fourth power of the peak current density, a 30% increase in this parameter would reduce the target lifetime by over 60%. At J-PARC, another high power facility with a liquid metal target, the situation is significantly better. Their multiwire monitor sits much closer to the target and recent studies have demonstrated agreement between this device and image plate activation analysis [2]. During commissioning at the SNS, the situation was also better. A temporarily installed Al2O3:Cr screen provided a full 2 dimensional image of the beam at the target [3]. This uncooled device was removed in 2006 before high power operation began. Due to the valuable data provided by the temporary system, and in anticipation of high power levels, a new beam on target imaging system is being developed.

IMAGING OPTIONS

Several sources of photons were considered. Their relative yields were calculated and are summarized in Table 1. In this table, the screen refers to a typical Chromium doped alumina material that was used in the temporary target imaging system. For the future, one option is to install a similar screen for low power tune-up after each target replacement. Before the pulse repetition rate is ramped up to achieve full power, the target would have to be retracted, the screen robotically removed, and the target reinserted. This procedure could take over one week and therefore impact operations.

Since a water-cooled shroud surrounds the target, a second option is to coat this shroud with a thin luminescent material. Heating of the scintillator would be limited, and it could be used during full power operations. As this option was selected for the initial deployment, it receives a detailed treatment in the next section.

Optical transition radiation is produced at the unmodified target surface. For 1 GeV protons, photon

07 Hadron Accelerator Instrumentation

yield is very low, but still may produce a detectable signal. Helium at a pressure of one atmosphere surrounds the target, leading to another source of photons. Excited by energy deposition from the incoming protons, this 99.9% pure gas will scintillate primarily in the shorter wavelengths of the visible spectrum. Helium fills the 2-meter long flight path between the target face and the proton beam window (which separates this region from the upstream accelerator vacuum). Therefore, to measure an accurate beam profile, optics with a shallow depth of field must be employed. Table 1 shows the estimated photon yield from a 10 mm thick slab of gas. When other sources are used to image the beam, Helium scintillation from a much thicker section could contribute a noticeable background.

At LANL in July of 2008, experiments were performed to observe both OTR and He scintillation with an 800 MeV proton beam. For this experimental configuration, a single pulse of $2.7 \cdot 10^{13}$ protons should have produced $3 \cdot 10^{8}$ visible photons within the imaging system's acceptance. Unfortunately, this initial test did not produce a discernable image. This was primarily due to two factors. The experiment was performed parasitically to a target test experiment and this led to severe constraints on the optical performance. In addition, a high gamma dose caused large background in the camera system. Follow-on experiments are anticipated.

Not shown in the table is the option of thermal incandescence. The most relevant example of this technique is employed for the SINQ target at PSI [4]. Although the light intensity is not proportional to beam current density, the system's sensitivity to off-normal conditions makes it an excellent input to a machine protection system.

Table 1: Photon Yields from the 1 GeV SNS Beam

Source	Photon Yield (photons/proton/steradian)
Screen (Cr:Al2O3)	$2*10^{+2}$
Coating (Cr:Al2O3)	$2*10^{+1}$
Optical Transition Radiation	$3*10^{-4}$
Helium scintillation (10 mm)	$3*10^{-3}$

Coating Development

Due to some early success and a tight schedule, a flame-sprayed Al2O3:Cr coating has been selected for the first replacement targets. During the LANL experiment mentioned above, several coating samples were tested and the results are shown in Fig. 2. To understand these results and further develop the coating process, collaboration was forged between SNS, ORNL's Material Science and Technology Division, and SUNY Stony Brook's Center for Thermal Spray Research.

Samples were analyzed with X-Ray diffraction and electron microscopy to determine the coating structure. These results were correlated with luminescent intensity measured by laser spectroscopy. UV excitation, and in some cases, proton beam excitation. The samples that

were flame sprayed with large particle sizes retain enough alpha phase alumina to efficiently scintillate. Higher temperature and velocity processes (D-gun and plasma spray) fully melt the particles and produce a less porous coating, but would require an undesirable high temperature anneal to restore the alpha phase. With the goal of depositing a functional coating without overheating the expensive target assemblies, the collaboration continues to map the parameter space of material properties and spray conditions.
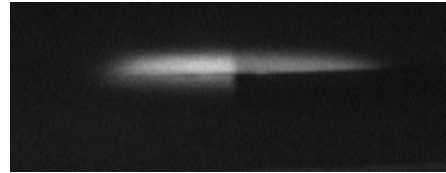
Figure 2: Test at LANL. Lower right quadrant: D-gun coating. Other quadrants: lower temperature flame sprayed coatings. Upper left: 1% Chromia. Upper right: 5% Chromia. Lower left: 0.5% Chromia.

At high beam power, the peak target surface temperature could approach 150 degrees C. Because the luminescent efficiency and decay time constant are both temperature dependant, gated imaging is being explored to simultaneously measure the beam profile and the temperature distribution.

OPTICAL SYSTEM
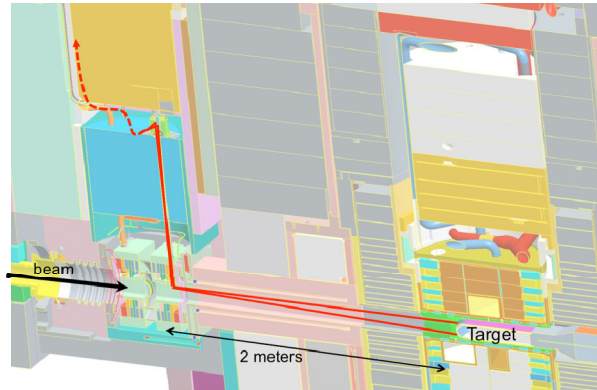
Figure 3: Optical path. Solid lines depict the reflective path and the dotted line depicts the beginning of the 11.5 meter long fiber bundle.

Imaging System Description

The proton beam imaging system was designed around a 25 mm viewport that extends 1.1 m vertically through a shielding plug above the proton beam window (PBW). A convex diamond-turned aluminum mirror mounted to the top surface of the proton beam flight tube (Fig. 4) serves as the input aperture of the imaging system.

The image from the convex mirror is reflected upward through the viewport, to a 45-degree flat diamond-turned aluminum mirror, that directs the light into a custom high-purity fused silica triplet lens. The turning mirror and lens are housed in a robust optics block securely mounted to the top of the PBW shielding plug (Fig. 4). The image

07 Hadron Accelerator Instrumentation

from the triplet lens is formed on the front face of an 11.5 m high-purity fused silica fiber optic imaging bundle (10,000 fibers) that terminates in a custom C-mount lens for attachment to a digital camera.
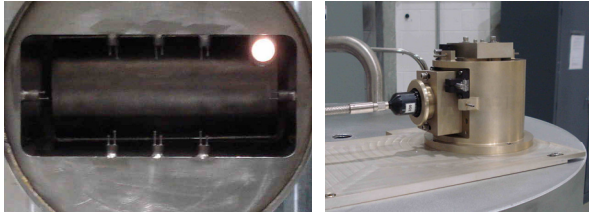
Figure 4: Left: Parabolic imaging mirror in PBW, reflecting viewport (illuminated). Right: Optics block, located 1 meter above parabolic mirror, with imaging lens and imaging fiber attached

Imaging System Design Considerations

The imaging system was designed to ensure that the necessary field of view would be preserved in the presence of several alignment uncertainties. In addition, the imaging fiber bundle was a long-lead-time item being manufactured in parallel with the other design activities and the manufacturer's specification on the input aperture of the fiber was nominally 1.1 mm with a +/- 10% tolerance. The design of the imaging system was based on the minimum fiber aperture of 1.0 mm with the goal of producing an image that was about 35% smaller than the minimum fiber diameter, to account for various alignment uncertainties. If the fiber were delivered at nominal aperture diameter (as expected) this margin would increase to about 42%. The resolution of the imaging system would be dictated by the projected size of the individual fiber elements. At the nominal fiber aperture diameter, the projected diameter of each individual imaging fiber onto the surface of the scintillator target would be 2.5 mm.

The use of an off-axis aspheric mirror as the input optic for the imaging system was motivated by field of view and imaging performance considerations but produced some distortion in the raytrace models (Fig. 5).
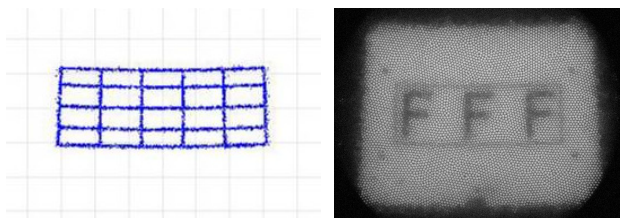
Figure 5: Left: optical modelling result showing anticipated image distortion. Right: Imaging system test target showing region of interest bounded by rectangle.

The optical throughput of the system is a function of the geometric loss from the scintillator to the input aperture, geometric loss within the imaging system itself, reflective losses at each optical element, packing fraction loss at the fiber and attenuation within the fiber itself. When all of these were taken into consideration, the system loss from the scintillator to the camera was calculated as 69 dB.

Imaging System Performance

Measurements of the assembled optical system were conducted using imaging targets with the 70 mm by 200 mm region of interest bounded by a rectangular border. The images produced (example shown in Fig. 5) indicated that the image was about 42% smaller than the fiber aperture, suggesting that the fiber bundle was delivered at near nominal diameter and that the resulting field of view is about 9.5°. The image geometry correlates reasonably well with the predicted distortion from the optical model, as shown in Fig. 5. Optical throughput of the system was measured using an illuminated integrating sphere at the object plane of the system with the output of the C-mount lens coupled into a silicon detector/amplifier. The optical loss was found to be approximately 65 db, which correlates well with the calculated loss of 69 db.

OUTLOOK

Installation of the optics and coating of a new target are both scheduled for Summer of 2009. Although significant risk remains, the goal is to achieve pulse by pulse imaging during the next run. An R&D program will continue to support development of more advanced coatings and optical components. Other applications are also under consideration.

ACKNOWLEDGEMENTS

REFERENCES

[1] B. Riemer, et. al, "Cavitation Damage Experiments for Mercury Spallation Targets at the LANSCE – WNR in 2005", Proc. Spallation Materials Technology 8, Taos, NM, October 2006.

[2] S. Meigo, et al., "Beam Commissioning of Spallation Neutron and Muon Source at J-PARC", Proc. PAC 2009, Vancouver (2009).

[3] T. J. McManamy, et. al., "SNS Target Viewscreen Design and Operation", AccApp 2007 Conference, Pocatello, UT (2007).

[4] K. Thomsen, "VIMOS, Beam Monitoring for SINQ", these proceedings (2009).